ORIGINAL ARTICLE
Turk J Surg

Incidental identification of elastofibroma dorsi in oncologic PET/CT imaging: a retrospective single-center analysis

Nilüfer Bıçakcı[1], Fatih Batı[2], Güler Silov[2], Banu Kırtıloğlu[1]

[1]Department of Nuclear Medicine, University of Health Sciences Türkiye, Samsun Training and Research Hospital, Samsun, Türkiye
[2]Department of Nuclear Medicine, Samsun University Faculty of Medicine, Samsun, Türkiye

ABSTRACT

Objective: To evaluate the morphological and metabolic characteristics of incidentally detected elastofibroma dorsi (EFD) on F-18 florodeoksiglukoz (FDG) positron emission tomography/computed tomography (PET/CT) and their longitudinal changes in oncologic patients.

Material and Methods: We retrospectively reviewed 42 197 PET/CT scans performed at our institution between January 2019 and September 2023. EFD was incidentally identified in 20 patients (0.05%). Patient demographics, primary malignancy, lesion localization, dimensions, and maximum standardized uptake values (SUV_{max}) were recorded. Measurements were obtained before treatment and at the next 3-month follow-up. Statistical analyses included Mann-Whitney U, Shapiro-Wilk and Spearman correlation tests; significance was set at $p<0.05$.

Results: The cohort comprised 17 females (85%) and 3 males (15%) with a median age of 67 years (range, 47-83). Primary diagnoses were breast cancer (n=8, 40%) and various other malignancies (n=12, 60%). Lesions were bilateral in 75% of cases. Pre-treatment lesion size ranged from 10 to 55 mm; median SUV_{max} was 2.4 (right) and 2.5 (left). No significant differences in baseline size or SUV_{max} were observed between breast and other cancers. A moderate correlation existed between right and left SUV_{max} ($r=0.641$; $p=0.010$). After 3 months, only the left longest diameter showed a statistically significant decrease (median, 45.0 mm vs. 43.0 mm; $p=0.034$), which may reflect measurement variability or positional factors rather than true biological change. SUV_{max} values remained stable.

Conclusion: Incidentally detected EFD on PET/CT exhibits low to moderate and stable FDG uptake and predominantly bilateral localization. Recognition of its characteristic features can prevent unnecessary interventions.

Keywords: F-18 FDG PET/CT, elastofibroma dorsi, SUV_{max}, incidental tumor, oncologic imaging

INTRODUCTION

The integration of positron emission tomography/computed tomography (PET/CT) with F-18 fluorodeoxyglucose (F-18 FDG) is a valuable functional imaging technique in oncology. Initially a research tool, the fusion of PET with CT to create PET/CT facilitated its widespread clinical adoption, offering substantial diagnostic capabilities (1). This modality is crucial in oncological management, encompassing initial diagnosis, staging, restaging, treatment planning, and patient monitoring. Indeed, F-18 FDG PET/CT is routinely employed for these purposes in numerous malignancies (2). However, it is important to recognize that F-18 FDG uptake is not specific to malignant processes. As F-18 FDG is not tumor-specific, its accumulation can also occur in infectious and inflammatory conditions. Nevertheless, malignant lesions, unlike most benign lesions, often exhibit sustained tracer retention during delayed imaging phases (3). This non-specificity can lead to diagnostic challenges, as various benign conditions that demonstrate F-18 FDG uptake can mimic malignancy. For instance, tuberculosis and other granulomatous diseases such as sarcoidosis can exhibit F-18 FDG avidity comparable to that of malignant tissues, posing diagnostic difficulties (4). Elevated F-18 FDG uptake can also be seen in specific physiological states and in various benign lesions, with such benign uptake being reported in over 25% of patients undergoing PET/CT examinations.

Elastofibroma dorsi (EFD) is a benign soft-tissue neoplasm typically located in the inferior subscapular region. Although typically found there, EFD has also been documented in other locations, including the axilla, ischial tuberosity, greater

Cite this article as: Bıçakcı N, Batı F, Silov G, Kırtıloğlu B. Incidental identification of elastofibroma dorsi in oncologic PET/CT imaging: a retrospective single-center analysis. *Turk J Surg.* [Epub Ahead of Print]

Corresponding Author
Fatih Batı
E-mail: fatih.bati@samsun.edu.tr
ORCID ID: orcid.org/0000-0003-3241-6417

Received: 26.05.2025
Accepted: 01.07.2025
Epub: 11.07.2025

DOI: 10.47717/turkjsurg.2025.2025-5-18

Available at www.turkjsurg.com

trochanter, elbows, and rarely, the stomach, rectum, and omentum. EFD was initially described in 1961 as a slow-growing pseudotumor characterized by the proliferation of fibroblasts and the accumulation of abnormal elastic fibers (5). The reported incidence of EFD varies considerably depending on the age of the population and detection methods. Autopsy studies indicate an EFD prevalence of 7-24% in women and 11-17% in men (6,7). Furthermore, pre-elastofibroma-like morphological changes, including degenerated elastic fibers, have been noted in up to 81% of autopsy cases (7). In a study of 258 patients undergoing chest CT for unrelated reasons, EFD was identified in 2% of patients (8).

The patients with EFD are predominantly asymptomatic. Symptomatic individuals may present with shoulder pain or a palpable, enlarging soft-tissue mass (9,10). Diagnosis is often incidental and is made via CT or magnetic resonance imaging (MRI), based on characteristic imaging features (11). On CT, EFD typically appears as a lenticular, non-encapsulated mass with attenuation similar to adjacent muscle, interspersed with hypodense striations corresponding to entrapped adipose tissue (12).

F-18 FDG PET/CT is an established tool for staging, restaging, monitoring therapy response, and prognostic stratification of diverse malignancies. Its applications range from common adult cancers to pediatric malignancies, where it aids in evaluating treatment efficacy and guiding therapeutic decisions (13). Early identification of treatment-resistant diseases using non-invasive methods, such as PET/CT, is of considerable clinical importance, facilitating timely adjustments to treatment strategies (14). Nevertheless, the literature on F-18 FDG PET/CT characteristics of EFD is primarily confined to sporadic case reports (15,16). Notably, beyond static descriptions, a significant knowledge gap exists regarding potential temporal changes in EFD appearance on sequential PET/CT scans. Elucidating this temporal evolution is essential for accurately differentiating benign EFD from tumor progression, particularly in oncological patients. Therefore, this study aimed to address this gap by evaluating the longitudinal F-18 FDG PET/CT features of incidentally detected EFD in oncologic patients.

MATERIAL and METHODS

Patients

This retrospective, single-center investigation reviewed all 42,197 oncologic F-18 FDG PET/CT scans performed at our institution between January 2019 and September 2024, among which EFD was incidentally identified in 20 patients (incidence rate: 0.05%). Demographic data, primary malignancy classifications, anatomical localizations of the EFD, lesion dimensions, and maximum standardized uptake values (SUV_{max}) values were documented. This investigation exclusively evaluated patients with incidental detection of EFD on F-18 FDG PET/CT.

We obtained approval for this study from the Samsun University Ethics Committee (ethics committee approval no: GOKAEK 2025/2/18, date: 24.01.2025).

F-18 FDG PET/CT Imaging

PET/CT scans were obtained 60 minutes after the injection using an integrated scanner (Philips Medical Systems, USA). All patients fasted for a minimum of 6 hours prior to the intravenous administration of 5 MBq/kg F-18 FDG. The pre-injection blood glucose levels were measured to ensure that they were below 200 mg/dL. During the distribution phase, patients remained in a supine position in a quiet room. Initially, an unenhanced CT scan with 5 mm slice thickness from the base of the skull to the inferior border of the pelvis was performed using a standardized protocol (140 kV and 80 mA). Subsequently, the PET scan was acquired from the base of the skull to the inferior border of the pelvis (8-10 bed positions, 1.5 minutes per bed position) without repositioning the patient on the table. The patient was permitted to breathe normally during PET and CT acquisitions. F-18 FDG PET images were reconstructed with CT-based attenuation correction.

Statistical Analysis

Semiquantitative evaluation of the PET component images was conducted by measuring SUV_{max} to assess the metabolic activity of the EFD. EFD size was determined using the longest and shortest diameters of the transaxial CT component images.

All data were analyzed using STATA/MP v.16 software (StataCorp LLC, Texas, USA). The Shapiro-Wilk test was employed to assess normal distribution, and numerical variables were provided as median (25^{th}-75^{th} percentile) values. Accordingly, Mann-Whitney U test was used to compare the two groups. The association between numerical variables was evaluated using Spearman's correlation analysis, and post-treatment changes were analyzed using the Wilcoxon test. Significance was accepted at $p<0.05$ (*) for all statistical analyses.

RESULTS

A total of 20 EFD patients were analyzed. The cohort included 17 females (85%) and 3 males (15%), with an age range of 47 to 83 years. The most common primary diagnosis among patients was breast cancer (8 patients, 40%), followed by endometrial cancer (3 patients, 15%) and ovarian cancer (3 patients, 15%). The EFD lesions were bilateral in most cases (75%). Initial lesion size ranged from 10 mm to 55 mm. The SUV_{max} values were low (range: 2.0 to 6.8), typically falling between 2.0 and 3.0 (Table 1). F-18 FDG PET/CT findings revealed bone metastases were present in 3 patients (15%), while cervical and axillary lymph node metastases were observed in 3 patients (15%). One patient with malignant melanoma exhibited a subcutaneous hypermetabolic density in the left medial region (5%). One patient with ovarian carcinoma had multiple peritoneal metastatic nodes (5%). Notably, 12

Table 1. Characteristics of patients with incidentally detected elastofibroma dorsi

Patient	Age	Gender	Primary diagnosis	Localization	Size before treatment (mm)	SUV_{max} before treatment	PET/CT findings	Size after treatment (mm)	SUV_{max} after treatment
1	79	Female	Breast	Left	10×55	Left: 2.9	Normal	-	-
2	64	Female	Breast	Right	15×45	Right: 2.2	Bone & Cervical lymph node metastasis	-	-
3	62	Female	Breast	Bilateral	Right: 11×52	Right: 2.1	Bone metastasis	Right: 10×50	Right: 2.0
					Left: 12×45	Left: 2.7		Left: 12×43	Left: 2.5
4	68	Female	Myelodysplastic syndrome	Bilateral	Right: 40×52	Right: 2.4	Normal	Right: 38×52	Right: 2.5
					Left: 35×50	Left: 2.1		Left: 33×48	Left: 2.0
5	80	Female	Breast	Bilateral	Right: 40×51	Right: 2.1	Bone metastasis	Right: 41×50	Right: 2.2
					Left: 35×45	Left: 2.7		Left: 35×45	Left: 2.6
6	67	Female	Endometrium	Bilateral	Right: 32×43	Right: 2.5	Normal	Right: 30×44	Right: 2.5
					Left: 41×51	Left: 2.4		Left: 39×50	Left: 2.5
7	77	Male	Lung	Left	40×52	Left: 2.3	Cervical lymph node metastasis	-	-
8	69	Female	Colon	Right	17×35	Right: 2.6	Recurrence	-	-
9	83	Female	Breast	Bilateral	Right: 37×55	Right: 3.0	Right axillary lymph node metastasis	Right: 38×56	Right: 3.0
					Left: 33×45	Left: 2.6		Left: 33×44	Left: 2.5
10	63	Female	Endometrium	Bilateral	Right: 44×35	Right: 2.8	Normal	Right: 42×35	Right: 2.8
					Left: 40×52	Left: 2.9		Left: 38×50	Left: 2.9
11	64	Male	Ovarian	Bilateral	Right: 35×43	Right: 3.1	Multiple peritoneal metastatic nodules	Right: 34×43	Right: 3.1
					Left: 38×42	Left: 2.9		Left: 38×40	Left: 2.7
12	64	Female	Endometrium	Bilateral	Right: 26×43	Right: 2.1	Normal	Right: 25×40	Right: 2.0
					Left: 34×35	Left: 2.3		Left: 34×37	Left: 2.2
13	71	Female	Colon	Bilateral	Right: 34×43	Right: 2.1	Normal	Right: 32×41	Right: 2.0
					Left: 35×39	Left: 2.2		Left: 34×38	Left: 2.1
14	65	Female	Breast	Bilateral	Right: 42×46	Right: 2.5	Normal	Right: 42×44	Right: 2.3
					Left: 40×42	Left: 2.4		Left: 41×42	Left: 2.5
15	47	Female	Breast	Right	34×58	Right: 2.3	Normal	-	-
16	69	Female	Liposarcoma	Bilateral	Right: 37×39	Right: 3.0	Normal	Right: 38×40	Right: 2.9
					Left: 35×37	Left: 2.7		Left: 34×36	Left: 2.6
17	58	Male	Malignant melanoma	Bilateral	Right: 40×42	Right: 2.4	Subcutaneous hypermetabolic densities in the left medial femur	-	-
					Left: 41×44	Left: 2.5			
18	64	Female	Ovarian	Bilateral	Right: 43×45	Right: 6.8	Normal	Right: 43×45	Right: 2.0
					Left: 45×47	Left: 4.5		Left: 45×47	Left: 2.1
19	66	Female	Ovarian	Bilateral	Right: 43×45	Right: 2.0	Normal	-	-
					Left: 45×47	Left: 2.1			
20	69	Female	Breast	Bilateral	Right: 43×45	Right: 2.4	Normal	-	-
					Left: 45×47	Left: 2.5			

PET/CT: Positron emission tomography/computed tomography, SUV_{max}: Standardized uptake values

patients (60%) had no metastatic involvement based on the F-18 FDG PET/CT findings (Table 1).

Prior to treatment, the mean lesion size was not significantly different between breast cancer and other cancers (Figure 1). Similarly, no association was observed between pre-treatment SUV_{max} values and demographic characteristics. Furthermore, there was no statistically significant correlation between lesion size and SUV_{max} values (Table 2).

Analysis of lesion size and metabolic activity before and after treatment revealed slight reductions in lesion dimensions (Table 1), although statistical significance was observed only in specific cases (Table 3). Notably, left-sided lesions showed a significant decrease in longest size after treatment (45.0 vs. 43.0 mm; p=0.034), while SUV_{max} values remained unchanged (Table 3).

Table 2. Demographic and imaging parameters associated with SUV_{max}

Variables	**SUV_{max}**			
	Right	**p**	**Left**	**p**
Age	r=-0.52[a]	0.854	r=-0.259[a]	0.351
Gender	2.4 (2.1-2.8)[b]		2.5 (2.3-2.7)[b]	
Female		0.476		
Male	2.7 (2.4-3.1)[b]		2.7 (2.5-2.9)[b]	0.477
Primary diagnosis	2.4 (2.1-2.5)[b]		2.6 (2.5-2.7)[b]	
Breast		0.679		0.680
Others	2.5 (2.1-3.0)[b]		2.5 (2.2-2.9)[b]	
PET/CT findings	2.5 (2.1-2.8)[b]	0.999	2.4 (2.2-2.7)[b]	0.165
Normal				
Abnormal	2.4 (2.1-3.0)[b]		2.7 (2.6-2.7)[b]	
Shortest dimension				
Right	r=0.188[a]	0.502	r=0.145[a]	0.606
Left	r=0.159[a]	0.571	r=0.003[a]	0.992
Longest dimension				
Right	r=-0.193[a]	0.491	r=-0.170[a]	0.544
Left	r=0.090[a]	0.749	r=0.060[a]	0.832
SUV_{max}				
Right	-	-	r=0.641[a]	0.010*
Left	r=0.641[a]	0.010*	-	-

Data were shown as median (IQR) or correlation coefficient. *: Indicates statistical significance at p<0.05, [a]: Spearman's rank correlation, [b]: Mann-Whitney U test, *: p<0.05, PET/CT: Positron emission tomography/computed tomography, SUV_{max}: Standardized uptake values, IQR: Interquartile range

Table 3. Change of size and SUV_{max} parameters after treatment

Variable	**Before**	**After**	**p**
Shortest dimension			
Right	40.0 (34.0-43.0)[d]	38.0 (31.0-41.5)[d]	0.087
Left	38.0 (35.0-41.0)[d]	34.5 (33.5-38.5)[d]	0.295
Longest dimension			
Right	45.0 (43.0-51.0)[d]	44.0 (40.5-51.0)[d]	0.067
Left	45.0 (42.0-47.0)[d]	43.0 (39.0-46.0)[d]	0.034*
SUV_{max}			
Right	2.4 (2.1-3.0)[d]	2.4 (2.0-2.9)[d]	0.299
Left	2.5 (2.3-2.7)[d]	2.5 (2.2-2.6)[d]	0.201

Data were shown as median (IQR), *: Indicates statistical significance at p<0.05, [d]: Wilcoxon signed-rank test for paired comparisons, SUV_{max}: Standardized uptake values, IQR: Interquartile range

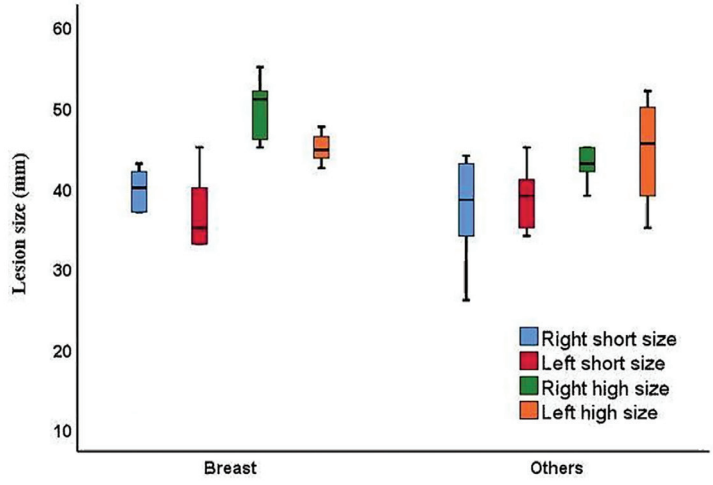

Figure 1. Box plots illustrating the distribution of elastofibroma dorsi lesion dimensions (mm) before oncologic treatment in patients with breast cancer (n=8) versus other primary malignancies (n=12). Within each main group, plots show the distribution for four different measurements: The right shortest dimension (labeled "Right short size"), the left shortest dimension (labeled "Left short size"), the right longest dimension (labeled "Right high size"), and the left longest dimension (labeled "Left high size"). Boxes indicate the interquartile range (IQR), the horizontal line represents the median, and whiskers typically extend to 1.5 times the IQR or the data range if within these limits.

DISCUSSION

EFD is a slow-growing benign connective tissue tumor that is most commonly located in the subscapular region of elderly individuals, particularly in females. With the increasing use of F-18 FDG PET/CT in oncologic imaging, incidental detection of EFD has become more frequent (5). In our study, 20 patients with incidentally detected EFD on PET/CT were analyzed. The majority were female (n=17, 85%), with an age range of 47 to 83 years and bilateral involvement was observed in 15 patients (75%). The predominance of female patients in this cohort is consistent with previous studies reporting a higher prevalence and frequent bilateral occurrence of EFD in elderly women, potentially attributable to hormonal or biomechanical influences (7,17). However, the FDG uptake observed in EFD lesions may pose a diagnostic dilemma, as it can mimic metabolically active malignant lesions. This study evaluated the characteristics of incidentally detected EFD lesions on oncologic F-18 FDG PET/CT, analyzed their temporal treatment-related metabolic behavior, and discussed their clinical implications.

Metabolic Activity and Other Imaging Characteristics

The SUV_{max} values of EFD lesions in our cohort ranged from 2.0 to 6.8, with a median SUV_{max} of 2.4 for the right site and 2.5 for the left sites (Figure 2). Literature findings support the observation that EFD generally exhibits low to moderate FDG uptake, but with a stable metabolic profile over time (9).

EFD, while benign, can mimic other soft tissue masses on imaging, necessitating careful evaluation to avoid misdiagnosis and unnecessary intervention (18). The potential for misclassification highlights the necessity of integrating clinical findings with imaging characteristics and, when uncertainty persists, pursuing tissue diagnosis to definitively exclude malignancy. A comprehensive diagnostic approach, moving beyond SUV_{max} alone, is essential to overcome the diagnostic challenge posed by variable F-18 FDG uptake in EFD. This involves the meticulous integration of key clinical indicators (such as older age, female predominance, and often asymptomatic presentation) with specific imaging patterns. Crucially, the high incidence of bilaterality, observed in 75% of our cohort, has emerged as a powerful diagnostic clue that strongly favors EFD over typically unilateral malignant lesions. When these clinical factors and the robust finding of bilaterality are combined with the characteristic morphological features on CT, the diagnostic confidence for EFD can be significantly increased, often obviating the need for invasive procedures in cases with typical presentations. Ultimately, an accurate diagnosis relies on a combination of imaging features, clinical context, and pathological correlation when necessary, which requires awareness of entities such as low-grade fibromyxoid sarcoma, which can present diagnostic challenges (19). It is essential to note that MRI excels in delineating soft-tissue lesions, relying solely on imaging studies for a definitive histological diagnosis is accurate in only a minority of cases (20). Thus, familiarity with the imaging characteristics of EFD is crucial for radiologists and nuclear medicine physicians to ensure the accurate interpretation of F-18 FDG PET/CT scans in oncologic patients. On CT imaging, EFD typically appears as a lenticular, non-encapsulated lesion with hypodense striations interspersed within the muscular tissue, corresponding to alternating fibrous and fatty components (12). On PET/CT imaging, EFD demonstrates low-to-moderate FDG uptake commonly within the 2.0-3.0 SUV_{max} range, which can help

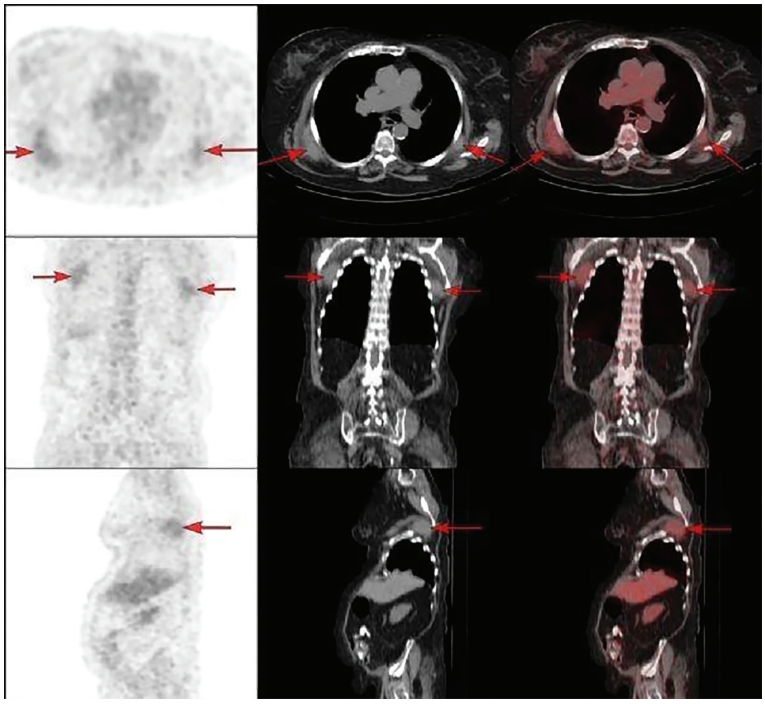

Figure 2. A 67-year-old female patient with a diagnosis of endometrial cancer underwent F-18 FDG PET/CT follow-up, which incidentally revealed findings consistent with elastofibroma dorsi (right SUV_{max}: 2.50- left SUV_{max}: 2.40). The condition manifested as mildly hypermetabolic uptake in soft tissue density within both subscapular regions (red arrows). (From top to bottom; axial, coronal, sagittal and left to right F-18 FDG PET, CT and F-18 FDG PET/CT fusion images are presented).

FGD: Florodeoksiglukoz, SUVmax: Standardized uptake values, PET/CT: Positron emission tomography/computed tomography

distinguish it from malignant soft tissue involvement (15,16). These imaging features are crucial in differentiating EFD from malignancies, particularly in oncological patients where soft tissue metastases or sarcomas are a major concern (11).

In our study, lesion sizes ranged from 10 mm to 55 mm, with a median diameter of 45 mm observed bilaterally. However, no statistically significant correlation was found between lesion size and SUV_{max} values, suggesting that the metabolic activity of EFD is not solely volume-dependent but may be influenced by underlying histological characteristics such as stromal composition or vascularity. Importantly, 60% of the patients in our cohort exhibited no evidence of metastatic disease, emphasizing the need for caution in interpreting incidental soft tissue findings in oncologic imaging.

Collectively, these observations support the interpretation of EFD as a benign, degenerative fibroblastic process rather than a hypermetabolic neoplastic entity (7). Nevertheless, in the differential diagnosis of soft tissue lesions such as EFD, a structured approach is essential, particularly to distinguish between neoplastic and non-neoplastic entities. In this context, the World Health Organization's 2013 classification of soft tissue tumors serves as a valuable framework for guiding clinical decision-making, including the appropriate use of biopsy in diagnostically uncertain cases (21).

Pre- and Post-treatment Changes

Few studies have evaluated longitudinal metabolic changes in EFD using F-18 FDG PET/CT (22). In our study, serial 18 F-FDG PET/CT scans revealed no significant changes in SUV_{max} values before and after oncologic treatment ($p>0.05$). In our study, a statistically significant reduction was observed in the longest diameter of left-sided EFD lesions following oncologic treatment, although the absolute magnitude of change was minimal (median: 45.0 mm to 43.0 mm; $p=0.034$). While this dimensional decrease may be incidental, it raises the possibility of subtle structural remodeling in response to systemic therapy or positional factors. Interestingly, existing literature, including the case series by Erhamamci et al. (23), does not report spontaneous or treatment-associated reduction in lesion size, instead focusing on static lesion characteristics and surgical outcomes. This discrepancy may reflect differences in patient selection (symptomatic vs. oncologic surveillance populations), imaging follow-up intervals, or underlying biological behavior. Although elastofibromas are generally considered metabolically and structurally stable, our findings suggest that minor variations in lesion size can occur over time, warranting cautious interpretation. Further prospective imaging studies are needed to determine whether such dimensional changes are reproducible and clinically relevant, or simply represent

measurement variability, mechanical influences, or postural shifts during imaging acquisition.

Study Limitations

This study acknowledges several limitations. Firstly, its retrospective design intrinsically poses risks of selection bias and incomplete clinical documentation. Secondly, as a single-center study, the generalizability of our findings may be constrained by institutional imaging protocols, equipment variations, and patient population characteristics. Thirdly, the relatively small sample size (n=20) limits the statistical power of subgroup analyses, particularly concerning treatment-related changes.

Additionally, the diagnosis of EFD was based solely on imaging characteristics without histopathologic confirmation, which, while ethically justified in typical cases, limits definitive validation. In clinical practice, biopsy is not routinely performed for incidentally detected EFD with classic imaging findings; however, histological confirmation remains essential in atypical or diagnostically equivocal presentations.

Lastly, variations in treatment regimens and follow-up intervals among patients precluded standardized assessment of temporal changes in lesion behavior, thereby limiting conclusions regarding the potential impact of oncologic therapy on EFD morphology or metabolism. Future studies with a prospective design, larger cohorts, and histologic correlation are warranted to address these limitations and to better define the natural course of EFD in oncologic populations.

CONCLUSION

EFD is characterized by its bilateral subscapular localization, low-to-moderate FDG avidity, and stable metabolic behavior as observed on PET/CT, which supports its benign nature. The integration of morphologic and metabolic findings enhances diagnostic specificity and reduces unnecessary interventions. Future research should prioritize the development of standardized imaging criteria and the study of longitudinal behavior to refine oncologic interpretation.

Ethics

Ethics Committee Approval: We obtained approval for this study from the Samsun University Ethics Committee (ethics committee approval no: GOKAEK 2025/2/18, date: 24.01.2025).

Informed Consent: Retrospective study.

Footnotes

Author Contributions

Data Collection or Processing - B.K.; Analysis or Interpretation - F.B.; Literature Search - G.S.; Writing - N.B.

Conflict of Interest: No conflict of interest was declared by the authors.

Financial Disclosure: The authors declared that this study received no financial support.

REFERENCES

1. *Pösteki G, Güreşin A, Güler SA, Şimşek T, Cantürk NZ. Utility of positron emission tomography for determination of axillary metastasis of breast cancer. Turk J Surg. 2023;39:293-299.*
2. *Bıçakcı N. Diagnostic and prognostic value of F-18 FDG PET/CT in patients with carcinoma of unknown primary. North Clin Istanb. 2022;9:337-346.*
3. *Çınar A, Gençoğlu EA, Korkmaz M. Restaging colorectal cancer and PET/CT. Turk J Surg. 2013;29:76-80.*
4. *Silov G, Çankaya E, Karaçavuş S. Evaluation of diffuse lymphadenopathy via various quantitative PET/CT parameters. Hell J Nucl Med. 2023;26:47-56.*
5. *Jarvi O, Saxen E. Elastofibroma dorse. Acta Pathol Microbiol Scand Suppl. 1961;51(Suppl 144):83-84.*
6. *Järvi OH, Länsimies PH. Subclinical elastofibromas in the scapular region in an autopsy series. Acta Pathol Microbiol Scand A. 1975;83:87-108.*
7. *Giebel GD, Bierhoff E, Vogel J. Elastofibroma and pre-elastofibroma—a biopsy and autopsy study. Eur J Surg Oncol. 1996;22:93-96.*
8. *Yanarateş G, Fidan N. Elastofibroma dorsi detected incidentally on chest computed tomography: the prevalence and reporting rate in radiology reports. Cureus. 2023;15:e51280.*
9. *Davidson T, Goshen E, Eshed I, Goldstein J, Chikman B, Ben-Haim S. Incidental detection of elastofibroma dorsi on PET-CT: initial findings and changes in tumor size and standardized uptake value on serial scans. Nucl Med Commun. 2016;37:837-842.*
10. *García-Jarabo E, García-Rabanal D, Casas-Ramos P, Bravo-Jiménez B, Ramos-Ramos L, Ramos-Pascua LR. [Elastofibroma dorsi: diagnosis and follow-up in primary care]. Semergen. 2023;49:101977.*
11. *Köksal A, Tuğtağ-Demir B, Çankal F. Detailed analysis of elastofibroma dorsi cases detected incidentally on thorax CT. J Med Palliat Care. 2023;4:579-584.*
12. *Oliva MS, Smimmo A, Vitiello R, Meschini C, Muratori F, Maccauro G, et al. Elastofibroma dorsi: what's new? Orthop Rev (Pavia). 2020;12(Suppl 1):8708.*
13. *Bıçakcı N, Silov G, Bıçakcı Ü, Batı F, Kırtıloğlu B. Nuclear medicine approaches in the field of oncologic pediatric surgery and review of the risk factors for pediatric thyroid nodules. Surg Child. 2025;2:21-27.*
14. *Başoğlu T, Özgüven S, Özkan HŞ, Çınar M, Köstek O, Demircan NC, et al. Predictive value of 18F-FDG PET/CT indices on extensive residual cancer burden in breast cancer patients treated with neoadjuvant chemotherapy. Rev Esp Med Nucl Imagen Mol (Engl Ed). 2022;41:171-178.*
15. *Onishi Y, Kitajima K, Senda M, Sakamoto S, Suzuki K, Maeda T, et al. FDG-PET/CT imaging of elastofibroma dorsi. Skeletal Radiol. 2011;40:849-853.*
16. *Metser U, Miller E, Lerman H, Even-Sapir E. Benign nonphysiologic lesions with increased 18F-FDG uptake on PET/CT: characterization and incidence. AJR Am J Roentgenol. 2007;189:1203-1210.*
17. *Ngoy A, Tchalukov K, Pollock G, Thomson B, Nguyen C. The first-reported presentation of quadruple locations of elastofibroma dorsi: a case report and review of the literature. Cureus. 2023;15:e41425.*
18. *Bartocci M, Dell'Atti C, Meacci E, Congedo MT, Magarelli N, Bonomo L, et al. Clinical features, imaging findings, treatment aspects of elastofibroma dorsi and long-term outcomes after surgical resection. Eur Rev Med Pharmacol Sci. 2017;21:2061-2068.*

19. *Deveci MA, Özbarlas HS, Erdoğan KE, Biçer ÖS, Tekin M, Özkan C. Elastofibroma dorsi: clinical evaluation of 61 cases and review of the literature. Acta Orthop Traumatol Turc. 2017;51:7-11.*
20. *Nishio J, Nakayama S, Nabeshima K, Yamamoto T. Current update on the diagnosis, management and pathogenesis of elastofibroma dorsi. Anticancer Res. 2021;41:2211-2215.*
21. *Doyle LA. Sarcoma classification: an update based on the 2013 World Health Organization classification of tumors of soft tissue and bone. Cancer. 2014;120:1763-1774.*
22. *Blumenkrantz Y, Bruno GL, González CJ, Namías M, Osorio AR, Parma P. Characterization of elastofibroma dorsi with (18)FDG PET/CT: a retrospective study. Rev Esp Med Nucl. 2011;30:342-345.*
23. *Erhamamci S, Reyhan M, Nursal GN, Torun N, Yapar AF, Findikcioglu A, et al. Elastofibroma dorsi incidentally detected by (18)F-FDG PET/CT imaging. Ann Nucl Med. 2015;29:420-425.*